Journal of Applied Polymer Science

Ultrathin and nanofibers via room temperature electrospinning from trifluoroacetic acid solutions of untreated lignocellulosic sisal fiber or sisal pulp

Bruno V. M. Rodrigues, Elaine C. Ramires, Rachel P. O. Santos, Elisabete Frollini
Macromolecular Materials and Lignocellulosic Fibers Group, Center for Research on Science and Technology of BioResources, Institute of Chemistry of São Carlos, University of São Paulo, 13560-970 São Carlos São Paulo, Brazil
Correspondence to: E. Frollini (E-mail: elisabete@iqsc.usp.br)

ABSTRACT: Lignocellulosic sisal fiber (LSF) and sisal pulp (SP) were electrospun at room temperature from solutions in trifluoroacetic acid (TFA) prepared at concentrations of 2×10^{-2} g mL^{-1} and 3×10^{-2} g mL^{-1}, respectively. Scanning electron microscopy images of the electrospun LSF showed fibers with diameters ranging from 120 to 510 nm. The presence of defects decreased along with increasing the flow rate of the SP solution, which generated nanofibers and ultrathin fibers with diameters in the range of 40–60 (at 5.5 μL min^{-1}) up to 90–200 nm (at 65.5 μL min^{-1}). Despite the known ability of TFA to esterify the hydroxyl groups present in the starting materials, the Fourier transform infrared spectra indicated the absence of trifluoroacetyl groups in the electrospun samples. The thermal stability of the final materials proved suitable for many applications even though some differences were observed relative to the starting materials. This study demonstrated a feasible novel approach for producing nano/ultrathin fibers from lignocellulosic biomass or its main component, which allows for a wide range of applications for these materials. © 2015 Wiley Periodicals, Inc. J. Appl. Polym. Sci. **2015**, *132*, 41826.

KEYWORDS: biopolymers & renewable polymers; cellulose and other wood products; electrospinning

Received 25 May 2014; accepted 25 November 2014
DOI: 10.1002/app.41826

INTRODUCTION

In the last few decades, natural fibers, such as lignocellulosic fibers, have been employed in a wide range of applications and have provided a positive contribution to the environment and to the petroleum supply issue. These fibers are most commonly used in the textile field[1–3] and as a composite reinforcement.[4–7] Among the most known lignocellulosic fibers, lignocellulosic sisal is an excellent candidate for use as reinforcement in composite applications due to its high cellulose content. In addition, Brazil is the largest worldwide producer and exporter of sisal, and many applications of these fibers have been investigated in the last few decades to generate final products with high aggregated values.

In recent decades, the investigation of nano-sized materials has progressed significantly due to the generation of materials with outstanding properties that typically exhibit superior mechanical performance,[8] large surface area to volume ratio,[9] and a variety of surface functionalities.[10] In this context, many investigations have attempted to extract nanocellulose in its different forms (nanofibrils or nanocrystals) from lignocellulosic fibers and wastes.[11–13] In general, these nanomaterials are prepared from acid and/or mechanical treatments in the lignocellulosic biomass and exhibit the potential for application as reinforcements in nanocomposites.[11,13]

Although the electrospinning technique has gained importance as a versatile technique for preparing fibers at the sub-micro- and nano-scales during the last two decades,[14–17] there has been a notable lack of investigation of lignocellulosic biomass as an alternative raw material. Few studies have been published regarding the electrospinning of lignocellulosic biomass, and all of these studies were restricted to the utilization of alkali-treated biomass and the 1-ethyl-3-methylimidazolium acetate ionic liquid as solvent.[17,18] However, room temperature electrospinning of the native lignocellulosic biomass has not yet been reported.

Electrospinning at room temperature requires a solvent that readily volatilizes under this condition. Trifluoroacetic acid (TFA), which is a very strong organofluorine acid, is widely used in organic synthesis due to its high acid strength, high volatility, and miscibility with a wide range of organic solvents. Another important advantage offered by TFA is that it can be easily recovered at low operating

This article was published online on 7 Jan 2015. An error was subsequently identified. This notice is included in the online and print versions to indicate that both have been corrected 14 Jan 2015.

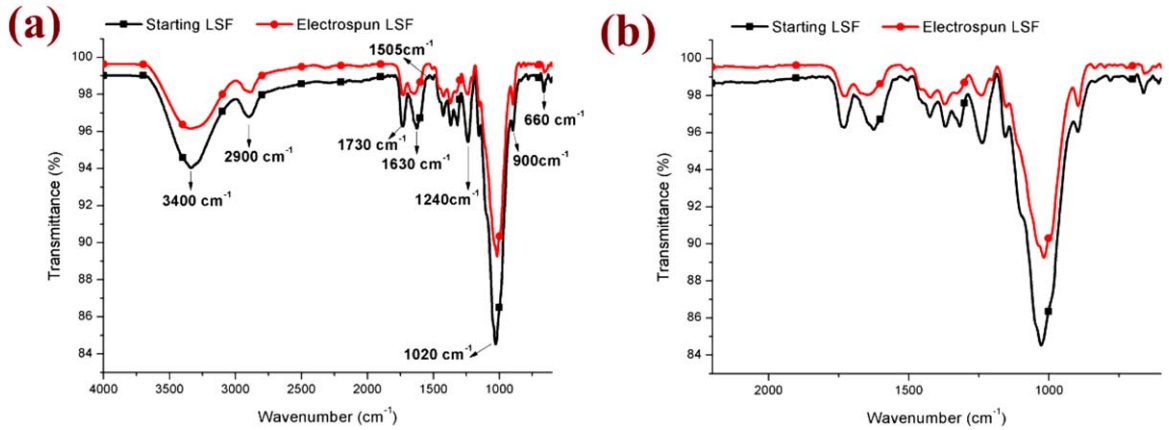

Figure 1. FTIR spectra of the starting and electrospun LSF (a) and zoom in the 2200–600 cm^{-1} region (b). [Color figure can be viewed in the online issue, which is available at wileyonlinelibrary.com.]

temperatures due to its low boiling point (72.4°C).[19,20] TFA has been used to disrupt cellulose crystallinity leading to the complete separation and dissolution of cellulose chains due to the nearly exclusive esterification of their hydroxyl groups at C6.[21] The trifluoroacetyl groups introduced into the cellulose chains are easily hydrolyzed by exposure to air after regeneration.[21,22]

The high content of cellulose in lignocellulosic sisal favors the spinnability of hemicelluloses, and particularly of lignin, when the three components of this fiber are subjected to electrospinning. Lignin, which is a component of lignocellulosic fibers, consists of a three-dimensional (3D) macromolecular network (protolignin), and its dissolution requires breaking covalent bonds to disrupt this 3D network. Fanta *et al.*,[23] who studied the hydrolysis of wheat straw with 1*N* TFA for 7 h, reported that both hemicellulose and lignin were degraded by 80% and 10%, respectively, while cellulose macromolecules remained largely unaffected after TFA dissolution.

Morrison and Stewart[24] compared the total sugar and reducing sugar of oat straw and cellulose TFA solutions during 1–16 days. After 8 days, the amount of the reducing sugar was higher for oat straw comparatively to the cellulose sample and increased significantly with time (while remained practically constant for cellulose). These results were primarily attributed to a depolymerization of noncellulosic polysaccharides (e.g., hemicelluloses) of oat straw.

In the current investigation, a novel approach to the room temperature electrospinning of native lignocellulosic biomass or its main component (i.e., cellulose) is reported. TFA was used to separate the components of the lignocellulosic fibers leading to the dissolution of cellulose, hemicellulose, and lignin. Subsequent reconstruction of fibers at sub-micro- and nano-scales was achieved by electrospinning.

To assess the influence of lignin and hemicellulose during the process of electrospinning, SP without lignin and with a low hemicellulose content was also used as a starting material. Because hemicellulose and lignin are strongly attached to the cellulose in the lignocellulosic fibrous structure, they hinder the motion of the cellulose chains in solution, which may influence both the jet and spinnability.

To the best of our knowledge, this is the first time that native lignocellulosic biomass-based ultrathin fibers have been prepared at

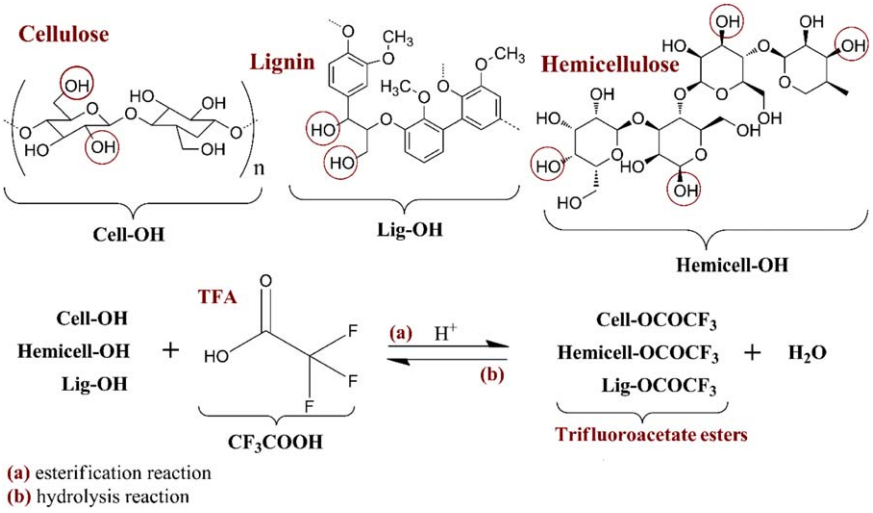

Figure 2. Main components of a lignocellulosic fiber: reactive sites susceptible to esterification by TFA. [Color figure can be viewed in the online issue, which is available at wileyonlinelibrary.com.]

room temperature by electrospinning using TFA as solvent. These ultrathin fibers may be used as membranes to prepare sandwich-type film structures or even to reinforce composites because the small diameters result in a high specific surface area up to 1000 times larger than that of the microfibers,[25,26] which allows direct contact between the cellulose chains and the polymer matrices.

EXPERIMENTAL

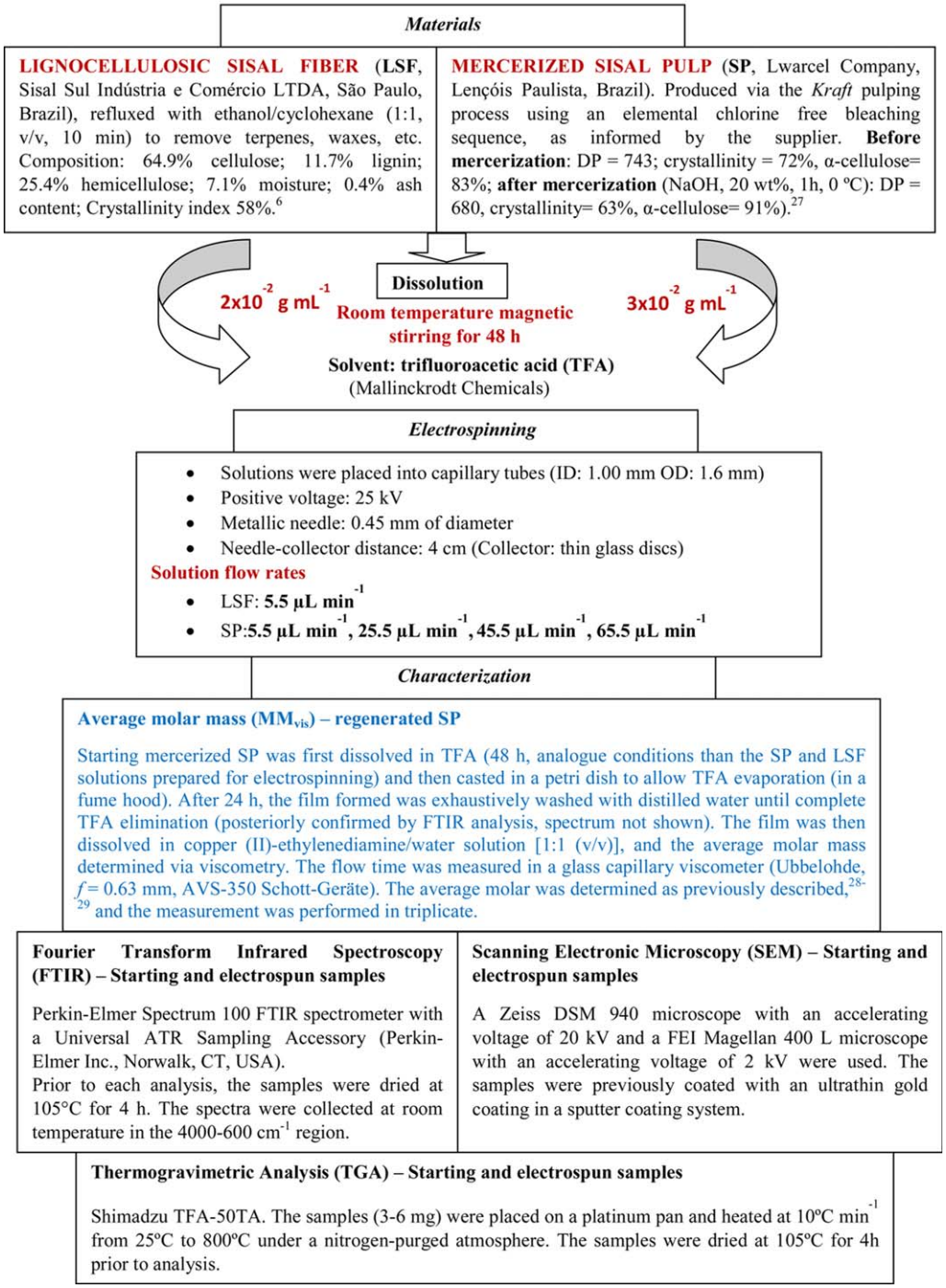

RESULTS AND DISCUSSION

FTIR

Figure 1 shows the FTIR spectra of the starting and electrospun LSF. The FTIR spectra for the starting and electrospun LSF (Figure 1) revealed characteristic peaks/bands of a typical lignocellulosic material. A band was observed at about 3400 cm^{-1}, which was attributed to O—H stretching. Additional bands involving O—H bending of adsorbed water at 1630 cm^{-1}, C—H stretching at

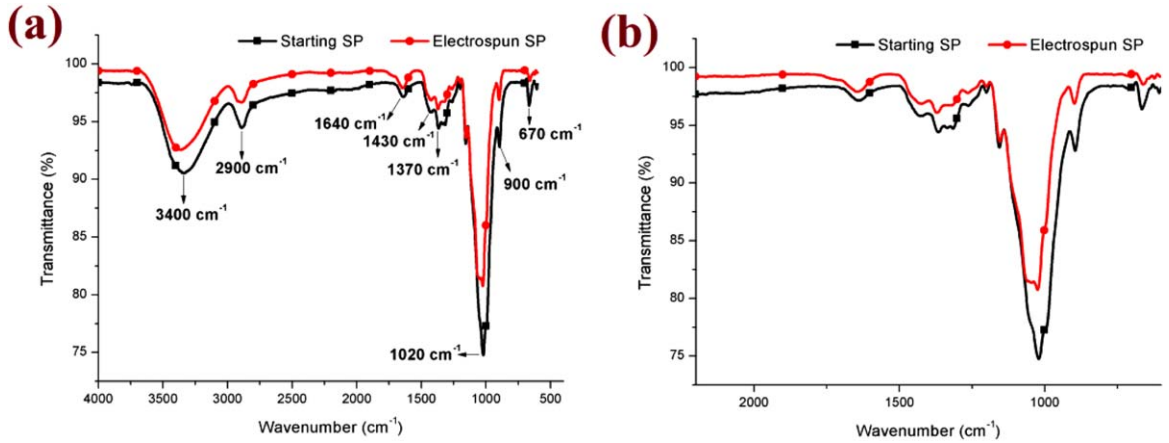

Figure 3. FTIR spectra of the starting and electrospun SP (a) and zoom at the 2200–600 cm^{-1} region (b). [Color figure can be viewed in the online issue, which is available at wileyonlinelibrary.com.]

2900 cm^{-1}, C—O stretching vibration of the cellulose backbone at 1020 cm^{-1}, C—O—C, C—C—O, and C—C—H deformation modes and stretching vibrations of the C-5 and C-6 atoms at 900 cm^{-1},[30] C–OH out-of-plane bending mode at 668 cm^{-1},[31] aromatic skeletal vibrations of lignin at 1505 cm^{-1}, and axial asymmetric strain of =C—O—C of lignin at 1240 cm^{-1} and C=O valence vibration of acetyl or COOH groups in the "xylan" components of hemicellulose at 1730 cm^{-1} were observed.

The hydroxyl groups of cellulose, hemicellulose, and lignin can be esterified by TFA (Figure 2), which may also act as an acid catalyst in this type of reaction. In this case, FTIR spectra with peaks in the region of 1790 cm^{-1} (absorption of the carbonyl of trifluoroacetyl groups) would be obtained.[21]

Montaño-Leyva *et al.*[22] reported the presence of the cellulose trifluoroacetate peak (1790 cm^{-1}) in the FTIR spectra of cellulose nanofibers prepared by electrospinning of TFA cellulose solutions. However, over the course of time and constant exposure to air (presence of humidity), spontaneous hydrolysis occurred, which led to the disappearance of the peak related to the ester carbonyl groups. Hasegawa *et al.*[21] also reported a decrease in the degree of substitution by trifluoroacetyl groups that were generated during cellulose dissolution due to the exposure of the regenerated cellulose to air. In the current study, the FTIR analysis of the electrospun LSF (Figure 1) was performed after drying the film at room temperature (2 days). The absence of peaks in the 1790 cm^{-1} region indicated that any trifluoroacetyl group coming from a possible esterification that may have occurred had been hydrolyzed on exposure to air.

Figure 3 shows the FTIR spectra of the starting and electrospun SP. The FTIR spectra for the starting and electrospun SP (Figure 3) exhibited characteristics peaks of a cellulosic material, such as the O—H stretching at about 3500 cm^{-1}, O—H bending of adsorbed water at 1640 cm^{-1}, C—H stretching at 2900 cm^{-1}, H—C—H and O—C—H— in-plane bending vibrations at 1430 cm^{-1}, the C—H deformation vibration at 1370 cm^{-1}, C—O stretching vibration of the cellulose backbone at 1020 cm^{-1}, C—O—C, C—C—O, and C—C—H deformation modes and stretching vibrations of the C-5 and C-6 atoms at 900 cm^{-1} [30] and C—OH out-of-plane bending mode at 668 cm^{-1}.[31] The FTIR spectrum for the electrospun SP exhibited no significant difference from the starting SP with no peaks in the region of 1790 cm^{-1}, which indicated the absence of trifluoroacetate groups after electrospinning followed by exposure to air.

Morphological Surface Analysis by Scanning Electron Microscopy

Figures 4 and 5 show the scanning electron microscopy (SEM) images of electrospun LSF and SP, respectively, at various solution flow rates. In contrast to SP (results discussed below), the solution flow rate for LSF was maintained constant at 5.5 μL min^{-1} because increasing the flow rate derailed the electrospinning process for LSF.

The SEM images of electrospun LSF (Figure 4) showed a homogeneous web of ultrathin LSF in a wide range of diameters (i.e., 120–510 nm) with an average diameter of 230 nm. This wide interval of diameters may be due to the presence of lignin in the lignocellulosic fiber, which may interfere in cellulose fibrillation by splaying leading to inefficient elongation via whipping motions to produce more uniform electrospun fibers.[17,18] In contrast to the results reported by Ahn *et al.*[17] and Kang *et al.*[18] for the electrospinning of alkali-treated hemp in ionic liquids, the electrospun LSF obtained herein exhibited a homogeneous web and smooth surface without "defects," such as bent fibers, knots, and filmogenic regions. It should be emphasized that to the best of our knowledge, this is the first time that a lignocellulosic fiber was electrospun without any fiber pretreatment, and TFA was used as solvent in the electrospinning of a lignocellulosic fiber.

The SEM images of electrospun SP (Figure 5) indicated that increasing the solution flow rate decreased the presence of defects across the fiber webs. Therefore, nanofibers (<100 nm) and ultrathin fibers were produced with diameters of 65–160, 90–165, and 90–200 nm using flow rates of 25.5, 45.5, and 65.5 μ L^{-1}, respectively. Previous studies, which also used TFA as solvent, reported nanofibers from cotton and wood pulp in the range of 30–50 nm[32] as well as ultrathin fibers from Durum Wheat Straw cellulose with diameters of approximately 270 nm.[22]

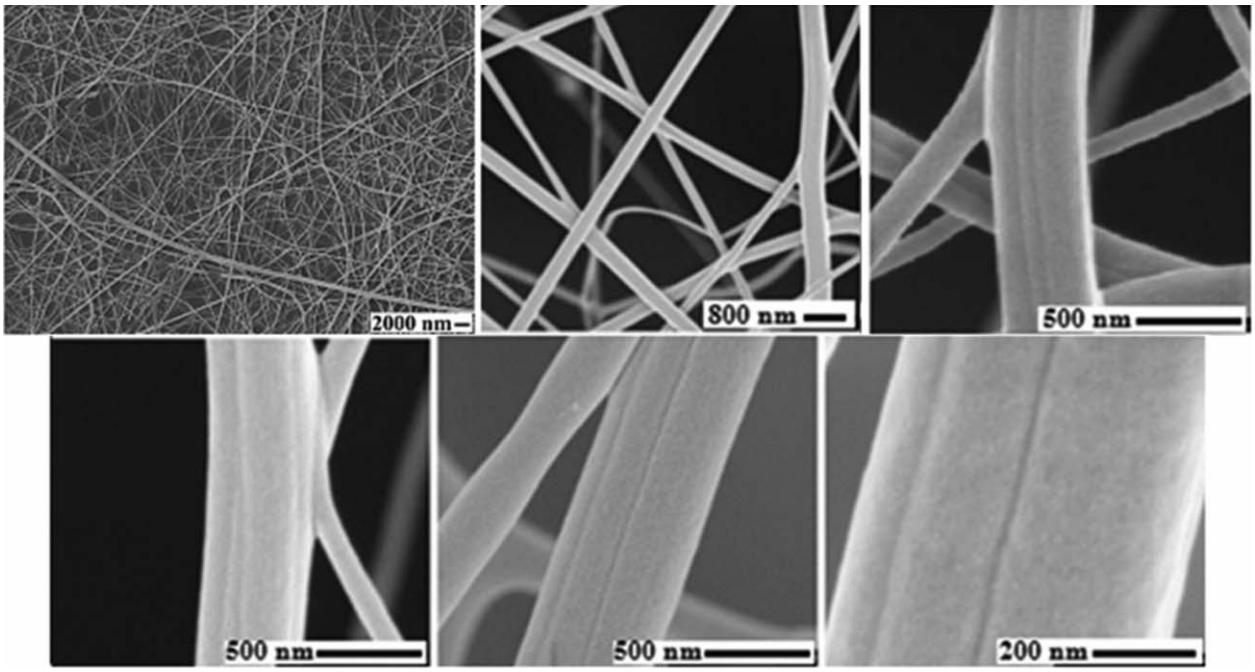

Figure 4. SEM images of electrospun LSF prepared at a constant solution flow rate (5.5 μL min^{-1}).

The jet/fiber diameter has a strict correlation with the flow rate.[33] According to empirical observations, an increase in the flow rate produces fibers with larger diameters[34–36] while maintaining the Taylor cone.[35–37] However, if the flow rate is too high to allow the necessary time for solvent evaporation from the fiber, a flattened web-like structure may be obtained. Therefore, a low flow rate is typically preferred while maintaining the Taylor cone because it slows for sufficient time for solvent evaporation and results in better and thinner fibers. Nevertheless, for the SP, the lowest flow rate (5.5 μL min^{-1}) resulted in a beaded fiber web with some flattened regions. This flow rate may have been below the threshold for the voltage used, which may have led to evaporation of the solvent at the needle, which caused instability of the jet during electrospinning.[38] Therefore, this flow rate led to the thinnest fibers (40–60 nm), but it also resulted in a flawed fiber web.

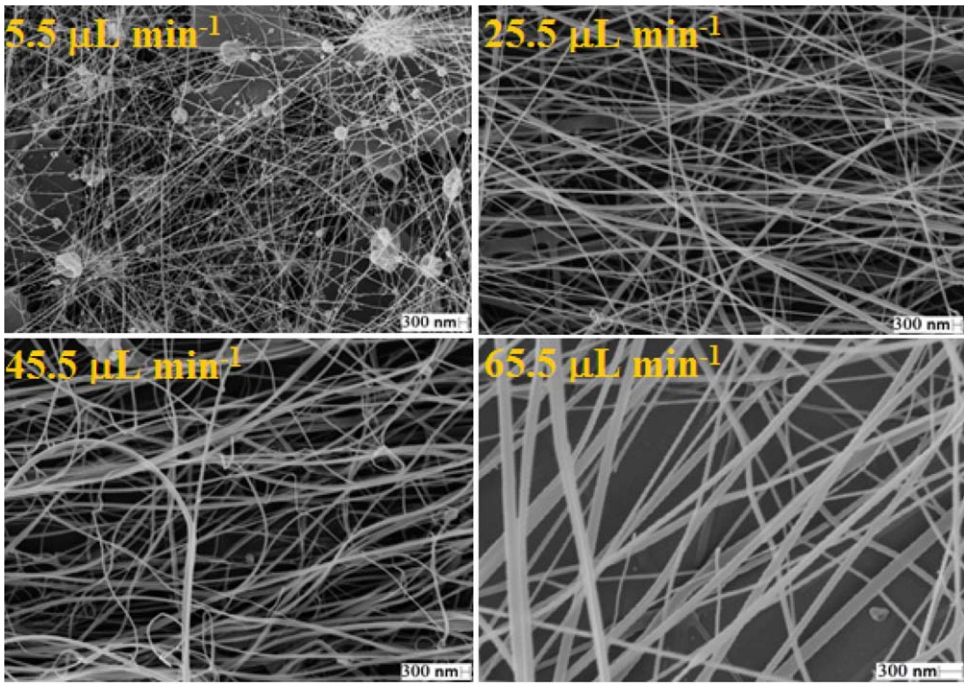

Figure 5. SEM images of electrospun SP prepared at various solution flow rates (5.5–65.5 μL min^{-1}). [Color figure can be viewed in the online issue, which is available at wileyonlinelibrary.com.]

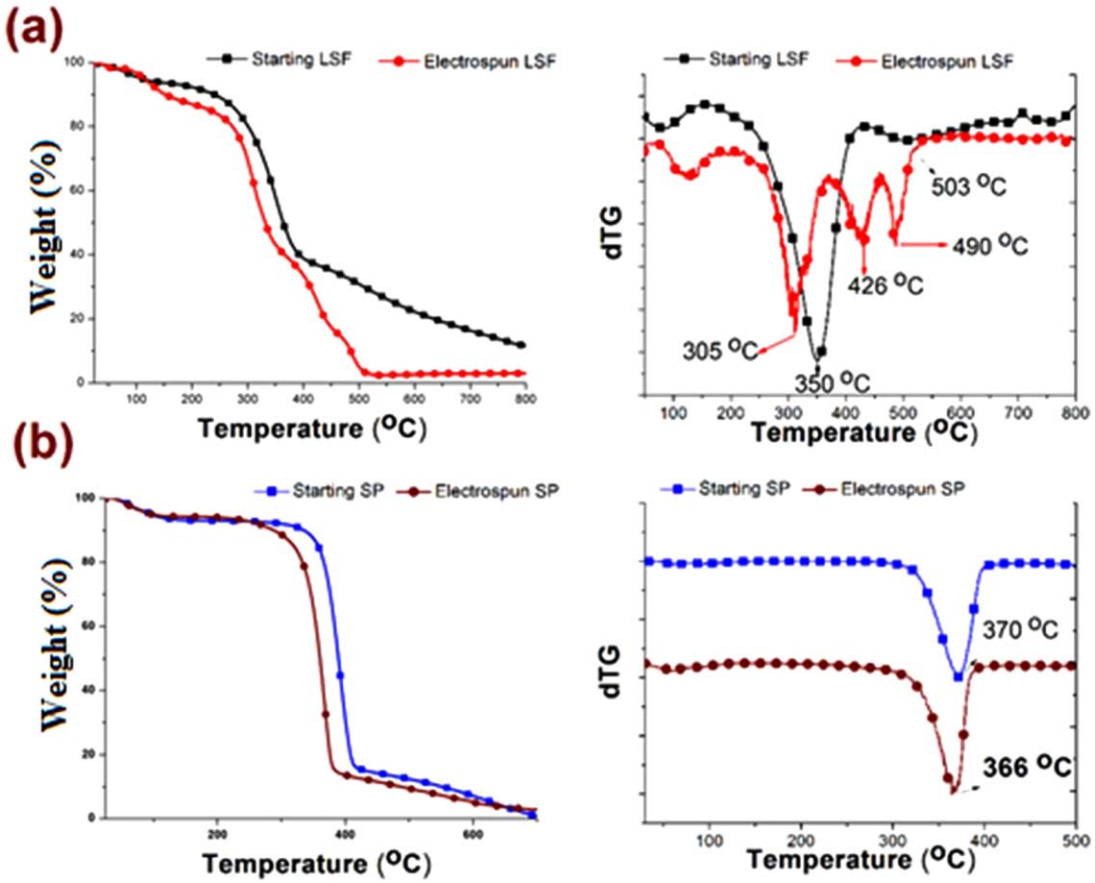

Figure 6. TG and dTG curves of (a) starting and electrospun LSF and (b) starting and electrospun SP (N_2 atmosphere at 20 mL min^{-1} and heating rate of 20°C min^{-1}). [Color figure can be viewed in the online issue, which is available at wileyonlinelibrary.com.]

Fong *et al.*[39] proposed that fiber formation is dependent on a combination of factors as follows: balance of forces caused by surface tension, solution viscosity and density of net charges on the jet. It should be mentioned that different concentrations of LSF and SP were used to determine the optimal conditions (e.g., viscosity) that lead to electrospinning for each one. The high viscosity of the LSF solution (at 2×10^{-2} g mL^{-1}), proved to be adequate for electrospinning. This LSF concentration was the threshold required to prevent solution gelification, and below this threshold, electrospinning was not possible under any of the tested conditions.

The viscometry results indicated a DP of 252 ± 1 for the regenerated SP (see Experimental section). This result indicated that the SP was partially hydrolyzed during dissolution in TFA (partial hydrolysis of hemicelluloses chains, followed by partial hydrolysis of the cellulose chains).[24] Consequently, the SP-TFA solution exhibited a lower viscosity than LSF at 2×10^{-2} g mL^{-1}, which was increased by raising the concentration to 3×10^{-2} g mL^{-1}, in order to allow for electrospinning. The higher viscosity of LSF compared to SP (at the same concentration, i.e., 2×10^{-2} g mL^{-1}) can be taken as an indication that, in the dissolution of LSF, the major action of TFA corresponded to the deconstruction of the lignocellulosic fiber and consequent release of lignin, hemicellulose, and cellulose to the solution.

Due to these differences in concentrations, the solution flow rate also required adjustments to optimize it for each solution. Therefore, only the lowest flow rate (5.5 μL min^{-1}) resulted in electrospinning of the LSF solution, and increases in the flow rate led to electrospraying.

Thermogravimetric Analysis

Figure 6(a) shows the TG and dTG curves for the starting and electrospun LSF. In the region of 75–125°C, the dTG curves of the starting and electrospun LSF (Figure 6) exhibited one peak, which was most likely related to the loss of water due to the moisture absorbed/adsorbed by the fiber[40] (mass loss of ca. 6% based on the TG curves). Most of the water molecules are bound to the hemicellulose chains present in the non-crystalline regions of the fiber. From 245°C to 380°C (Electrospun LSF) and from 245 to 420°C (Starting LSF) Figure 6(a) shows a weight loss of 52 and 46% (TG curves), respectively, and peaks (T_p) at 305°C and 350°C (dTG curves), respectively, which can be attributed to the decomposition of hemicelluloses followed by cellulose decomposition. The T_p values, which correspond to the maximum rate of mass loss, indicate that the electrospun LSF exhibited a lower thermal stability than the starting LSF.

The low intensity broad peak observed in the dTG curve of the starting LSF [Figure 6(a)] at 503°C corresponds to bond

breaking of the protolignin (native lignin). This peak characterizes the thermal decomposition of the lignin, which is the minor component of the sisal fiber (11.7%, see Experimental section). The aromatic structure of the lignin provides higher thermal stability to this macromolecule compared to cellulose. In comparison to the starting LSF, the TG curve of the electrospun LSF exhibited a different profile from 400°C, and two peaks were observed at 426°C and 490°C (dTG). Both peaks were attributed to the thermal decomposition of structures generated by the breakdown of protolignin during dissolution in TFA. As previously discussed, lignocellulosic fiber dissolution requires the breakage of covalent bonds to disrupt the lignin 3D network, which leads to the degradation of the protolignin. Therefore, the thermal decomposition of the structures generated by the protolignin breakdown was most likely responsible for the different behavior observed in both TG and dTG curves.

Similar TG and dTG curves were obtained for SP before (Starting SP) and after electrospinning (Electrospun SP) [Figure 6(b)]. Up to 125°C, a weight loss of about 6% was observed due to the absorbed/adsorbed water. Between 260°C and 420°C and 240 and 415°C, the starting and electrospun SP experienced a mass loss of 77 and 80%, respectively, which was due to cellulose depolymerization. According to the dTG curves [Figure 6(b)], the T_p values for the electrospun and starting SP were 366°C and 370°C, respectively. The decomposition of cellulose leads to the formation of levoglucosan (1,6-anhydro-β-D-glucopyranose), which is the primary product of cellulose pyrolysis.[41]

CONCLUSIONS

The current study has successfully introduced a new method for room temperature electrospinning of the lignocellulosic biomass using LSF as a starting material. TFA proved to be an excellent solvent for break down the lignocellulosic fibrous structure, which led to the separation of its main components. Using the electrospinning technique, the reconstruction of the lignocellulosic fibrous structure (LSF) generated ultrathin fibers with diameters ranging from 120 to 510 nm without any non-electrospun residues, as depicted in the SEM images. Electrospinning of the main component of the lignocellulosic fiber [i.e., cellulose (SP)] could also be performed at room temperature, and in addition to ultrathin fibers, nanofibers were produced. Some adjustments to the flow rate were necessary to obtain a more homogeneous and defect-free fiber web. Therefore, cellulose ultrathin and nanofibers were generated in a wide range of diameters as the solution flow rates were varied. These results open a wide range of possible applications in which lignocellulosic bio-based nano/ultrathin fibers may be used, such as *sandwich-type* structures of films, membranes or reinforcement in composite materials.

ACKNOWLEDGMENTS

The authors gratefully acknowledge FAPESP (The Sate of São Paulo Research Foundation, Brazil) for the fellowship for B.V.M.R. (proc. 2010/00005-4) and financial support as well as the CNPq (National Research Council, Brazil) for the research productivity fellowship for E.F. and financial support. They also wish to thank the Photochemistry Group (Institute of Chemistry of São Carlos, University of São Paulo), for the FTIR-ATR analyses.

REFERENCES

1. Kozlowski, R. M.; Muzyczek, M.; Mackiewicz-Talarczyk, M. *Adv. Mater. Res.* **2013**, *747*, 3.
2. Zimniewska, M.; Batog, J.; Bogacz, E.; Romanowska, B. *J. Fiber Bioeng. Inform* **2012**, *5*, 321.
3. Parikh, D. V.; Calamari, T. A.; Sawhney, A. P. S.; Blanchard, E. J.; Screen, F. J.; Myatt, J. C.; Muller, D. H.; Stryjewski, D. D. *Text. Res. J* **2002**, *72*, 668.
4. Oliveira, F. B; Gardrat, C; Enjalbal, C; Frollini, E; Castellan, A. *J. Appl. Polym. Sci.* **2008**, *109*, 2291.
5. Ramires, E. C; Frollini, E. *Compos. Part. B-Eng* **2012**, *43*, 2851.
6. De Oliveira Santos, R. P.; Castro, D. O.; Ruvolo-Filho, A.; Frollini, E. *J. Appl. Polym. Sci.* **2014**, *131*, 40386.
7. Satyanarayana, K. G.; Arizaga, G. G. C.; Wypych, F. *Prog. Polym. Sci.* **2009**, *34*, 982.
8. Ezatpour, H. R.; Sajjadi, S. A.; Sabzevar, M. H.; Huang, Y. *Mater. Des.* **2014**, *55*, 921.
9. Wang, X.; Pakdel, A.; Zhang, J.; Weng, Q.; Zhai, T.; Zhi, C.; Golberg, D.; Bando, Y. *Nanoscale Res. Lett.* **2012**, *7*, 662.
10. Ma, H.; Hsiao, B. S.; Chu, B. *J. Membr. Sci.* **2014**, *452*, 446.
11. Ghaderi, M.; Mousavi, M.; Yousefi, H.; Labbafi, M. *Carbohydr. Polym.* **2014**, *104*, 59.
12. Song, Q.; Winter, W. T.; Bujanovic, B. M.; Amidon, T. E. *Energies* **2014**, *7*, 607.
13. Chirayl, C. J; Mathew, L; Thomas, S. *Res. Adv. Mater. Sci.* **2014**, *37*, 20.
14. Reneker, D. H.; Chun, I. *Nanotechnology* **1996**, *7*, 216.
15. Maeda, N.; Miao, J.; Simmons, T. J.; Dordick, J. S.; Linhardt, R. J. *Carbohydr. Polym.* **2014**, *102*, 950.
16. Li, H.; Chen, H.; Zhong, X.; Wu, W.; Ding, Y.; Yang, W. *J. Appl. Polym. Sci.* **2014**, *131*, 40515.
17. Ahn, Y.; Lee, S. H.; Kim, H. J.; Yang, Y.-H.; Hong, J. H.; Kim, Y.-H.; Kim, H. *Carbohydr. Polym.* **2012**, *88*, 395.
18. Kang, Y.; Ahn, Y.; Lee, S. H.; Hong, J. H.; Ku, M. K.; Kim, H. *Fiber. Polym.* **2013**, *14*, 530.
19. Zhou, X. Q.; Cheng, B. B.; Huang, J. L.; Zhang, L. Y.; Lu, H. C.; Liao, L. Y. *Chin. J. Ener. Mater.* **2012**, *20*, 501.
20. Mahajan, Y. S.; Shah, A. K.; Kamath, R. S.; Salve, N. B.; Mahajani, S. M. *Sep. Purif. Technol.* **2008**, *1*, 58.
21. Hasegawa, M.; Isogai, A.; Onabe, F.; Usuda, M. *J. Appl. Polym. Sci.* **1992**, *45*, 1857.
22. Montaño-Leyva, B.; Rodriguez-Felix, F.; Torres-Chávez, P.; Ramirez-Wong, B.; López-Cervantes, J.; Sanchez-Machado, D. *J. Agric. Food Chem.* **2011**, *59*, 870.
23. Fanta, G. F.; Abbott, T. P.; Herman, A. I. *Biotechnol. Bioeng.* **1984**, *26*, 1122.
24. Morrison, I. M.; Stewart, D. *Phytochemistry* **1998**, *49*, 1555.
25. Li, D; Xia, Y. *Adv. Mater.* **2004**, *16*, 1151.

26. Huang, Z.-M; Zhang, Y. Z; Kotaki, M; Ramakrishna, S. *Compos. Sci. Technol.* **2003**, *63*, 2223.

27. Rodrigues, B. V. M.; Heikkilä, E.; Frollini, E.; Fardim, P. *Cellulose* **2014**, *21*, 1289.

28. Morgado, D. L.; Martins, V. C. A.; Plepis, A. M. G.; Frollini, E. *Polímeros* **2011**, *21*, 143.

29. TAPPI Test Method T 230 om-08. TAPPI Press: Atlanta, Georgia, **2008**.

30. Proniewicz, L. M.; Paluszkiewicz, C.; Wesełucha-Birczyńska, A.; Majcherczyk, H.; Barański, A.; Konieczna, A. *J. Mol. Struct.* **2001**, *596*, 163.

31. Schwanninger, M.; Rodrigues, J. C.; Pereira, H.; Hinterstoisser, B. *Vib. Spectrosc.* **2004**, *36*, 23.

32. Ohkawa, K; Hayashi, S; Nishida, A; Yamamoto, H; Ducreux, J. *Text. Res. J* **2009**, *79*, 1396.

33. Munir, M. M.; Suryamas, A. B.; Iskandar, F.; Okuyama, K. *Polymer* **2009**, *50*, 4935.

34. Homayoni, H.; Ravandi, S. A. H.; Valizadeh, M. *Carbohydr. Polym.* **2009**, *77*, 656.

35. Son, W. K.; Youk, J. H.; Lee, T. S.; Park, W. H. *J. Polym. Sci. Part B: Polym. Phys.* **2004**, *42*, 5.

36. Lim, Y.-M; Gwon, H. J; Jeun, J. P; Nho, Y. C. In Nanofibers; Ashok Kumar, Ed., InTech: Croatia, **2010**.

37. Yarin, A. L; Koombhongse, S; Reneker, D. H. *J. Appl. Phys.* **2001**, *90*, 4836.

38. Chowdhury, M; Stylios, G. *Int. J. Basic Appl. Sci.* **2010**, *10*, 8.

39. Fong, H.; Chun, I.; Reneker, D. H. *Polymer* **1999**, *40*, 4585.

40. Ornaghi, H., Jr; Poletto, M.; Zattera, A.; Amico, S. *Cellulose* **2014**, *21*, 177.

41. Morgado, D. L.; Frollini, E. *Polímeros* **2011**, *21*, 111.